Applied Catalysis B: Environmental 240 (2019) 215–224

Contents lists available at ScienceDirect

Applied Catalysis B: Environmental

journal homepage: www.elsevier.com/locate/apcatb

Oxidative denitrogenation with TiO_2@porous carbon catalyst for purification of fuel: Chemical aspects

Biswa Nath Bhadra, Ji Yoon Song, Nizam Uddin, Nazmul Abedin Khan, Sunghwan Kim, Cheol Ho Choi, Sung Hwa Jhung*

Department of Chemistry and Green-Nano Materials Research Center, Kyungpook National University, Daegu 41566, Republic of Korea

ARTICLE INFO

Keywords:
Denitrogenation
H_2O_2
Organonitrogen compounds
Oxidation
TiO_2

ABSTRACT

In order to investigate the possible denitrogenation of fuels, oxidation of organonitrogen compounds (ONCs) was carried out by using H_2O_2 green oxidant over a TiO_2-containing carbon catalyst, prepared by the pyrolysis of an MOF-composite [ZIF-8(30)@H_2N-MIL-125] (named as MDC-C). Neutral ONCs, including indole (IND) and its derivatives, especially those with high electron density on the nitrogen of the ONCs, different from basic ONCs, could be effectively oxidized, especially in the presence of a suitable extracting solvent CH_3COOH. MDC-C showed a high turnover frequency in the oxidation of IND as compared with various commercial or synthesized TiO_2 nanoparticles. The used catalyst could be recycled by simple solvent washing up to the fourth run without severe deactivation. Therefore, it could be confirmed that MDC-C is very effective in oxidative denitrogenation to remove ONCs, especially neutral ones, from fuels in the presence of H_2O_2 and a suitable extractant. Importantly, oxidation of IND derivatives was performed firstly under similar conditions in order to understand the mechanism of the reaction. The results showed that high electron density (that calculated in this study) on the nitrogen of the IND and its derivatives is very important, suggesting that the electrophilic addition of oxygen atoms onto the substrates (via N on the INDs) might play a crucial role in the oxidation, even though further study is essential to support this assumption.

1. Introduction

Fossil fuels are the most widely used energy resources in recent days, and their demand or exploration is increasing with the current technological advancements and the increasing population worldwide. To address this issue, new and unconventional fuel resources are being explored [1,2]. These raw fuels usually contain several contaminants including various organonitrogen compounds (ONCs) [3,4]. These ONCs are chemically active and thereby rust refinery equipment and block pipelines which are stringent problems in fuel processing technology [5–9]. Therefore, it is very important to remove such ONCs (similar to the removal of organosulfur compounds, OSCs [9–16]) from fossil fuels before utilization.

Hydroprocessing has been considered as one the effective and dominant ways to remove organo-sulfur compounds (OSCs) [17–19] and ONCs in fuel processing technologies, in which hydrodenitrogenation (HDN) of ONCs can be occurred simultaneously with hydrodesulfurization (HDS) of OSCs [20–23]. Moreover, HDN often has drawbacks, including high cost (because the HDN reaction spends expensive hydrogen), side reactions, and low efficiency. More importantly, removal of ONCs via hydrogenation requires ring hydrogenation (different from OSC removal), and therefore, HDN is carried out at high temperature and high pressure and requires much hydrogen. Solvent/acid extraction [24,25] and adsorption [8–11,26–30] have been proposed as alternatives to HDN for deep denitrogenation. Even though several adsorbents based on carbon [26,27,31], zeolites [28], silica [29], ion-exchange resins [30], and metal organic frameworks (MOFs) [9–14] are used in the adsorption of ONCs from fuels, it is still challenging to develop a highly efficient (can make N content < 1 ppm) adsorbent. Moreover, extraction and adsorption techniques are not yet in the stage of commercialization. Consequently, development of alternating methods for deep denitrogenation is still demanding to researchers as well as industrialists.

ONCs that are generally found in fossil fuels can be classified into two kinds: basic and non-basic (or neutral) compounds. Basic ONCs include quinoline (QUI), aniline, and their derivatives, and these can be removed relatively easily by the acid refining method via an acid-base reaction; however, the removal of non-basic compounds consisting of

* Corresponding author.
E-mail address: sung@knu.ac.kr (S.H. Jhung).

https://doi.org/10.1016/j.apcatb.2018.09.004
Received 18 June 2018; Received in revised form 11 August 2018; Accepted 2 September 2018
Available online 03 September 2018

pyrrole (PRL), indole (IND), carbazole (CBZ), and their derivatives is still challenging.

In recent years, oxidative desulfurization (ODS) [32–42] has been widely studied as a competitive method for the desulfurization of fuels. Oxidation or advanced oxidation is a very attractive method to solve environmental issues [43–45]. There are also a few reports on oxidative denitrogenation (ODN) [46–55]; however, so far, those studies have not been very systematic or detailed. Moreover, the progress of the studies on ODN is much slower as compared with that for ODS, possibly because of the different chemical nature of OSCs and ONCs. ONCs and OSCs consist of the second row element N and the third row element S, respectively. Different from S, which can be oxidized into sulfone or sulfoxide, nitrogen can seldom be oxidized into N oxides.

Therefore, it is quite challenging/fascinating to study the ODN of ONCs, especially non-basic ONCs, in order to find a highly effective method for the deep denitrogenation of fuels. Very recently, we developed a Ti-based catalyst (MDC-C) for ODS [56]. Inspired by the remarkable efficiency of MDC-C in the ODS process, we applied MDC-C in ODN to investigate the prospect of the ODN technology, especially with the MDC-C catalyst.

In this report, we investigated the ODN of IND (mainly) as a representative non-basic ONC using Ti-based heterogeneous catalysts and H_2O_2 as a green oxidant [57]. The ODN reaction was conducted with MDC-C systematically, including the study of the reaction kinetics under a wide range of reaction conditions and the effect of the extractant on the removal of IND. The MDC-C showed a fascinating performance (e.g., relatively low activation energy, fast kinetics or high turnover frequency, and good recyclability in ODN) as compared to some TiO_2 catalysts in the ODN. More importantly, oxidation of other ONCs such as PRL, CBZ, QUI and 1-, 2-, and 3-methyl-substituted INDs (1Me-IND, 2Me-IND, and 3Me-IND, respectively) was also conducted to suggest a plausible mechanism for the ODN process based on their relative reactivity, obtained products/intermediates, and electron densities (calculated in this study) on the N atoms of the substrates.

2. Experimental procedures

2.1. Materials

All materials were obtained from commercially available vendors and were used without further treatment. PRL (C_4H_5N, 99%), CBZ ($C_{12}H_9N$, 95%), IND (C_8H_7N, 99%), 1Me-IND (C_9H_9N, 97%), 2Me-IND (C_9H_9N, 98%), 3Me-IND (C_9H_9N, 98%), 2-methylimidazole ($C_4H_6N_2$, 98%) and P-25 (commercial TiO_2, product of Degussa) were purchased from Sigma-Aldrich. Titanium(IV) isopropoxide ($Ti[OCH(CH_3)_2]_4$, 97%), 2-aminoterephthalic acid ($C_8H_7O_4N$, 99%), and zinc nitrate hexahydrate ($Zn(NO_3)_2{\cdot}6H_2O$, 98%) were procured from Alfa Aesar. Acetonitrile (99%), methanol, *N,N*-dimethylformamide ($HCON(CH_3)_2$, 99%), formic acid, and acetic acid were obtained from OCI chemicals. *n*-Octane (C_8H_{18}, 97%) was acquired from Yakuri Chemical Co., Ltd. TiO_2 powder (anatase, 99%, called TiO_2(comm.) in this study), NaOH (96%), HCl (38%), hydrogen peroxide (H_2O_2, 30 wt%), and granular activated carbon (AC; 2–3 mm, practical grade) were procured from Duksan chemical Co.

2.2. Synthesis of the catalysts

The catalyst MDC-C was synthesized as per an earlier method [56] by pyrolyzing a prepared MOF composite [ZIF-8(30)@H_2N-MIL-125] in a tubular furnace (GSL-1500X-50-UL) equipped with a gas flow-through arrangement. To synthesize TiO_2 nanoparticle having anatase and rutile phases, reported methods [58,59] were followed; and the obtained products were named as TiO_2-A(synth.) and TiO_2-R(synth.), respectively. Furthermore, the TiO_2-R(synth.)@AC was prepared similarly via a simple impregnation method.

2.3. Characterization methods

The crystal phases of the studied materials were examined by an X-ray diffractometer (D2 Phaser, Bruker) equipped with Cu Kα radiation. The N_2 adsorption isotherms were measured at −196 °C with a surface area and porosity analyzer (Micromeritics, Tristar II 3020) after evacuation of the samples at 150 °C for 6 h. The Brunauer–Emmett–Teller (BET) method was adopted at a relative pressure of 0.05–0.20 to estimate the surface areas of the studied materials. Pore size was analyzed using Barrett-Joyner-Halenda (BJH) method. The morphologies, size, and distribution of the particles were judged using a field-emission transmission electron microscopy (FE-TEM; Titan G2ChemiSTEM Cs probe). Additionally, the chemical compositions (C, O, and N) were evaluated using elemental analysis (Thermo Fisher, Flash-2000 with a thermal conductivity detector), and the Ti and Zn contents were obtained using inductively coupled plasma (ICP)-optical emission spectrometry (Thermo Scientific Co., iCAP 6300 Duo).

2.4. Catalytic ODN experiments

The required amounts of IND, 1Me-IND, 2Me-IND, 3Me-IND, PRL, QUI, and CBZ were dissolved in *n*-octane to prepare model fuel solutions (5000 mg/L) in separate volumetric flasks. The oxidation of ONCs was conducted for 5–120 min in a single reaction vessel by the combined oxidation-extraction method. The extractant (2 mL of acetic acid, unless otherwise stated) in 20 mL of a model fuel solution (IND) was stirred at 50 °C in the presence of various amounts of 30% H_2O_2 (with the oxidant to nitrogen molar ratio (O/N) ranging from 0 to 15) and a fixed amount of catalyst (0.005 g). At first, the effect of mixing speed (rpm) was checked by stirring the reaction mixture from 100 to 1000 rpm for 120 min at 50 °C. Then, the effect of catalyst doses (ranging from 0 to 0.5 g/L of solution) was investigated at an O/N of 10.

Unless otherwise described, the reaction was done under a selected condition (catalyst: MDC-C; temperature: 50 °C; O/N: 10; mixing speed: 500 rpm; catalyst amount: 0.25 g/L). The oxidation of IND was also performed at two other temperatures (30 and 40 °C) using MDC-C to investigate the reaction kinetics at different temperatures and determine the activation energy of the catalysis. To investigate the effect of water on the oxidation of IND, the reactions were also conducted in the presence of 5–10 wt% of water in CH_3COOH using MDC-C catalyst. The oxidation of various ONCs, including INDs, PRL, QUI, and CBZ, was also investigated under the selected conditions. The effect of the extractive solvent on the oxidation of IND was also investigated by conducting ODN in MeCN, MeOH, and HCOOH, instead of acetic acid, with the catalyst MDC-C, under the mentioned conditions.

After the completion of the reaction for a preset time, the mixture was cooled to room temperature, and the liquid portion was separated by filtration using a syringe filter (polytetrafluoroethylene, hydrophobic, 0.5 μm). The oil or *n*-octane phase (non-polar) and extractive solvent phases (polar) were separated by a separatory funnel. The oil phase was analyzed to estimate the remaining amount or the conversion of ONCs using the UV-1800 system (Shimadzu) at 287, 285, 288, 290, 227, 313, and 291 nm for IND, 1Me-IND, 2Me-IND, 3Me-IND, PRL, QUI, and CBZ, respectively. The solutions were also analyzed with a gas chromatograph (GC; DS Science, IGC 7200) equipped with a flame ionization detector in order to further confirm the results measured by using UV absorbance. On the other hand, the oxidized products of IND, 1Me-IND, 2Me-IND, 3Me-IND, PRL, QUI, and CBZ that were extracted into the polar phase (CH_3COOH) were characterized with a gas chromatography mass spectrometer (GC–MS; Agilent, 7890A-5975C GC/MSD).

The used MDC-C catalyst was regenerated via simple soaking in acetone (1 L per g of used catalyst) under sonication for 1 h, and the recovered catalysts were used in the next cycle after subsequent evacuation at 100 °C overnight. The processes were continued up to the fourth cycle.

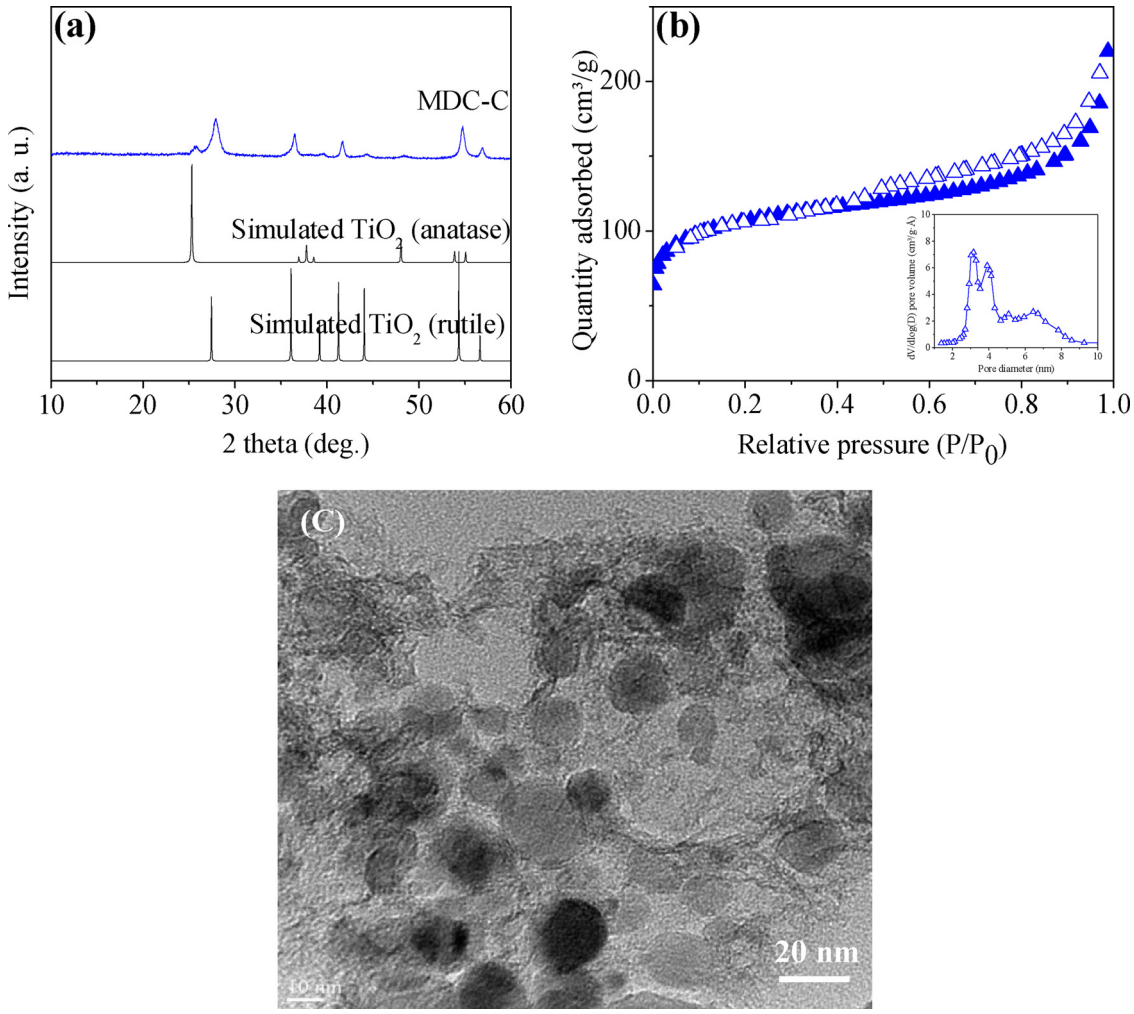

Fig. 1. (a) XRD pattern, (b) N_2-adsorption isotherm and (c) HR-TEM image of MDC-C. Simulated XRD patterns of anatase and rutile phases of TiO_2 were shown for comparison. Inset of the figure b shows the pore size distribution curve of MDC-C.

2.5. Method for the calculation of electron density and HUMO-LUMO gaps

The B3LYP/6-311 + + G(2d,2p) level of theory was employed for the geometry optimizations and electron density calculations of IND derivatives, PRL, QUI, and CBZ. The Mulliken population analysis method [60] was adopted for the calculation of the electron density of the optimized structures of the studied substrates. The MP2/aug-cc-pVTZ level of theory was used for the geometry optimizations and calculation of the $\Delta E_{HOMO\ -\ LUMO}$ gaps for PRL and benzene. The GAMESS program was used for all quantum mechanical calculations [61,62].

3. Results and discussion

3.1. Characterization of the catalysts

The X-ray diffraction (XRD) pattern (Fig. 1a) of the MDC-C showed that the catalyst is composed of rutile-TiO_2 (JCPDF No. 021-1276) as the main phase, with a small amount of anatase-TiO_2 (JCPDF No. 021-1272) [63]. However, the XRD patterns for both the synthesized [58] and commercial TiO_2 confirmed the phase-pure anatase $-TiO_2$ (Fig. S1a). Again, the XRD patterns (Fig. S1a) of the synthesized rutile $-TiO_2$ (also TiO_2-R(synth.)@AC, prepared via impregnation on AC) was corroborated with the rutile-TiO_2 (JCPDF No. 021-1276). Interestingly, MDC-C showed broader XRD peaks than those of TiO_2-A(synth.), TiO_2-A(comm.) and TiO_2-R(synth.), indicating that the TiO_2 particle size in MDC-C is the smallest among any TiO_2 including the commercial P-25. In detail, the average crystal sizes of the TiO_2 particles, estimated by using the Scherrer equation, in MDC-C, TiO_2-A(synth.), TiO_2-A(comm.) and TiO_2-R(synth.) and P-25 were about 8, 15, 52, 64, and 21 nm, respectively.

The textural properties of the studied materials were obtained from the N_2 adsorption isotherms (Fig. 1b, Figs. S1b, and S2). Even though the BET surface area of ZIF-8(30)@H_2N-MIL-125 (654 m^2/g) decreased upon pyrolysis, MDC-C showed a considerably higher surface area (374 m^2/g) than that of TiO_2-A(synth.) (139 m^2/g), TiO_2-A(comm.) (119 m^2/g), TiO_2-R(synth.) (96 m^2/g), and P-25 (40 m^2/g), as summarized in Table S1. Only TiO_2-R(synth.)@AC showed higher surface area (524 m^2/g) than that of MDC-C. In addition, the total, micro and mesopore volumes followed a similar order (MDC-C > TiO_2-A(synth.) > TiO_2-A(comm.) > TiO_2-R(synth.) > P-25) as their surface area (except TiO_2-R(synth.)@AC), where MDC-C showed the highest mesopore volume among all the studied materials. In addition, the BJH pore size analyses of MDC-C showed a wide range of mesopores (about 3 to 9 nm, as shown in the inset of Fig. 1b). Fundamentally, larger pores of heterogeneous/porous catalysts usually show more facile accessibility of the reactants to the active sites as well as higher reactivity of the substrate [64–66]. Moreover, the shape, size, and arrangement of TiO_2 nanoparticles supported on a carbon support were analyzed by FE-TEM (as shown in Fig. 1c). Other properties, including crystal morphology (FE-SEM images), Ti distribution (SEM- and TEM-EDS mapping), phases and degree of graphitization (Raman spectrum), and

functionalities (Ti, O, and N; XPS) of MDC-C, were explained in our previous report [56].

Therefore, TiO_2 nanoparticles (supported on mesoporous carbon with a considerably high surface area and large pores) might be a suitable catalyst for ODN, similar to the results of ODS [56]. Particularly, the smaller particle size and uniform shape of the nanoparticles is the fundamental avenues for the high-performance heterogeneous catalysts [67]. The other pure TiO_2 materials, synthesized and commercial ones, might be helpful for comparison (porous catalyst vs. non-porous catalyst) as well as for a better understanding of ODN reactions.

3.2. Catalytic oxidation of ONCs

At the very beginning, to rule out any possible diffusion limitation, an important factor of catalyses under porous heterogeneous catalysts, the effect of stirring speed (rpm) on the conversion of IND over the MDC-C catalyst was conducted. As illustrated in Fig. S3, the effects of stirring speed on the conversion showed a saturation of IND conversion at the 500 rpm when the reactions were carried out at 50 °C. Therefore, other ODN reactions were carried out under the selected reaction condition.

Oxidation of IND (a typical non-basic ONC) in *n*-octane solvent was conducted with the catalyst MDC-C at 50 °C for 120 min using CH_3COOH as the extractant and H_2O_2 as the green oxidant [57,68]. The UV and GC analyses of the oil phases showed no peak corresponding to IND; however, the GC–MS spectrum (Fig. S4a) of the polar phase showed the presence of two new peaks (P2 and P3) rather than that from IND. The products in the polar phase could be identified from the fragmentation patterns shown in Figs. S4b and c. The two products (P2 and P3) were identified as 1,3-dihydro-indol-2-one or 1,2-dihydro-indol-3-one (indoxyl) and 1H-indole-2,3-dione (isatin), respectively (structures are shown in each figure). Briefly, the obtained results revealed that IND was oxidized very effectively with MDC-C under the tested conditions.

Previously, a study on ODN with MoO_3/Al_2O_3 catalyst [48,69] suggested the formation of indoxyl in the first step and further oxidized into isatin with other polymerized materials. The observed results for the oxidation of IND in the two studies are in agreement with each other, even though the current results showed the formation of only two products without any polymerized materials. This difference might be because the reaction conditions, including the applied catalysts, are quite different from each other.

The effects of oxidant-to-nitrogen ratio (O/N) and catalyst dose on the oxidation of IND were further studied. Fig. 2 demonstrates the effects of O/N (Fig. 2a) and catalyst (MDC-C) dose (Fig. 2b) on the oxidation of IND under similar conditions (in the presence of *n*-octane, CH_3COOH, and H_2O_2 applied as the solvent, extractant, and oxidant, respectively). These results revealed that an O/N of 10 and 0.25 g/L of the catalyst might be the standard choice, and further investigation of the ODN reaction was performed under these conditions, unless otherwise stated.

After selecting the standard amounts of catalysts and O/N ratio, the oxidation of IND was investigated further by replacing CH_3COOH with MeCN, MeOH, or HCOOH (as an alternative extractant). The UV and GC analyses of the oil phases (excluding the polar phase with an extractant such as MeCN, MeOH, or HCOOH) showed the presence of remaining IND, even though the content was reduced from the initial conditions. Moreover, the GC–MS spectra (Fig. S5) of the polar phases showed the presence of IND as the main component with a trace amount of other products (P2 and P3). These results revealed that the removal of a considerable amount of IND is possible via extraction; however, simple solvent extraction (using MeCN, MeOH, or HCOOH) was inadequate for deep denitrogenation. As mentioned, both Fig. S5a (in MeCN) and S5c (in HCOOH) showed the corresponding peak for the reactant IND (Fig. S5d), whereas peaks P2 and P3 corresponded to oxidized INDs (observed similarly in the case of CH_3COOH applied as the extractant). In

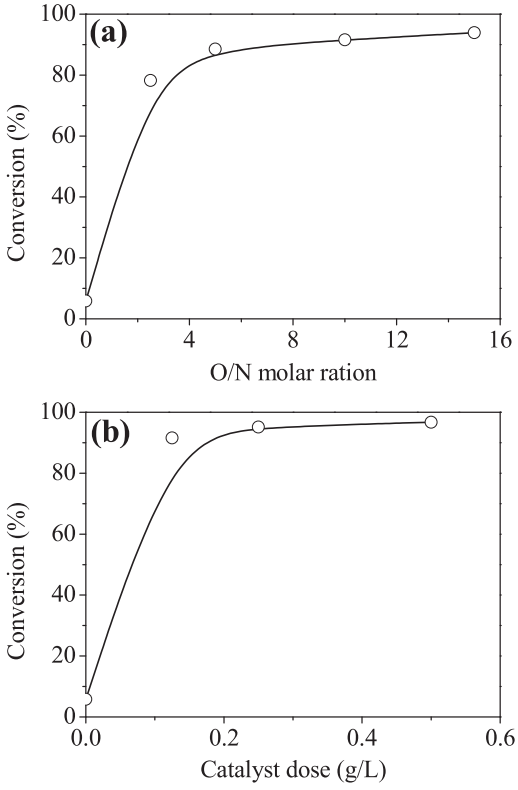

Fig. 2. Effect of the (a) O/N molar ration, and (b) catalyst doses on the oxidative removal of IND from n-octane. MDC-C and CH_3COOH was used as catalyst and extractant, respectively.

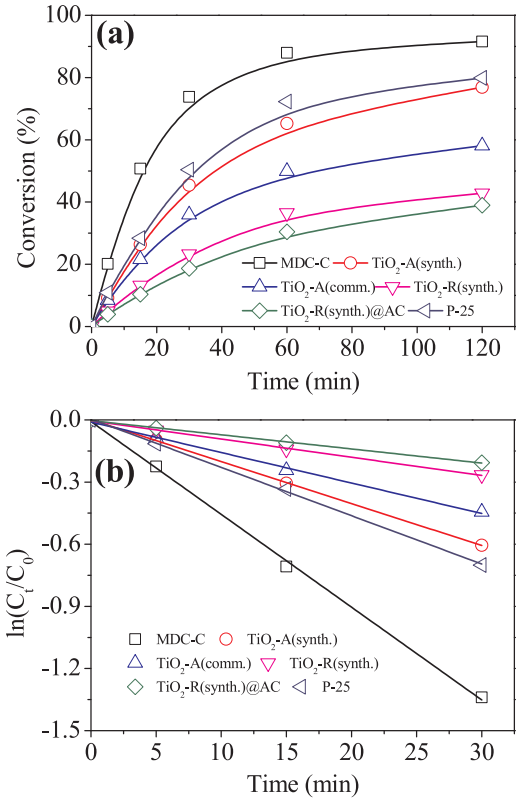

Fig. 3. Effect of reaction time on (a) IND conversion and (b) plots of the pseudo-first-order kinetics for the oxidation of IND over MDC-C, TiO_2-A(synth.), TiO_2-A(comm.), TiO_2-R(synth.), TiO_2-R(synth.)@AC, and P-25 at 50 °C.

Table 1
Pseudo-first-order rate constants and correlation factors for the oxidation of IND over MDC-C, TiO_2-A(synth.), TiO_2-A(comm.), TiO_2-R(synth.), TiO_2-R (synth.)@AC, and P-25 at 50 °C. Rate constants for the oxidation of Me-INDs, PRL and CBZ over MDC-C are also shown. TOF values of the IND oxidation are also listed.

Substrate	Catalyst	k (min^{-1})[b]	R^2 [c]	TOF (h^{-1})[d]
IND	TiO_2-A(synth.)	2.0×10^{-2}	0.960	12.5
	TiO_2-A(comm.)	1.4×10^{-2}	0.990	9.9
	TiO_2-R(synth.)	8.8×10^{-2}	0.986	6.4
	TiO_2-R(synth.)@AC	6.1×10^{-2}	0.991	9.1
	P-25	2.3×10^{-2}	0.995	13.7
	MDC-C	4.5×10^{-2}	0.997	30.7
	MDC-C (5 wt% H_2O)[a]	3.8×10^{-2}	0.994	
	MDC-C (10 wt% H_2O)[a]	2.8×10^{-2}	0.995	
1Me-IND	MDC-C	1.3×10^{-2}	0.998	
2Me-IND	MDC-C	3.0×10^{-2}	0.997	
3Me-IND	MDC-C	1.4×10^{-2}	0.987	
PRL	MDC-C	8.1×10^{-3}	0.988	
CBZ	MDC-C	1.9×10^{-3}	0.987	

[a] Added water was wt% of CH_3COOH.
[b] Rate constant.
[c] Correlation coefficient.
[d] Turn of frequency, which was calculated by the following equation:

the oxidation in the presence of CH_3OH extractant (Fig. S5b), two other peaks (P2″ and P3″) were observed along with the IND peak, which was quite different from the results in the presence of other extractants. Therefore, the obtained results might suggest that IND oxidation is quite complex and that the extractant plays a critical role in the oxidation reaction for ODN. Interestingly, CH_3COOH was the best choice as the extractant for the oxidation of IND among the studied extractants.

IND oxidation was conducted with different Ti-based catalysts, for a wide range of reaction times, in order to investigate the efficiency as well as competitiveness of the catalyst MDC-C in ODN. Fig. 3a compares the conversion of IND as a function of time over MDC-C, TiO_2-A(synth), TiO_2-A(comm.), TiO_2-R(synth.), TiO_2-R(synth.)@AC and P-25 (commercial product of Degussa). As shown in Fig. 3a, after completion of the ODN in a set time (120 min), MDC-C showed the highest conversion (92%) of IND. On the contrary, TiO_2-A(synth), TiO_2-A(comm.), TiO_2-R (synth.), TiO_2-R(synth.)@AC and P-25 showed relatively lower conversion (77%, 58%, 43%, 39% and 80% respectively) even though the Ti contents of these nanoparticles were higher than that of MDC-C (Table S1).

The kinetics of IND oxidation over MDC-C along with TiO_2-A(synth), TiO_2-A(comm.), TiO_2-R(synth.), TiO_2-R(synth.)@AC and P-25 was interpreted by applying a pseudo-first-order kinetic model. The rate constants (k) and correlation coefficients (R^2) observed from the kinetic plots (Fig. 3b) for IND oxidation over the tested catalysts are shown in Table 1. The R^2 of ~0.98 confirmed that the pseudo-first-order kinetic model could be used as an effective model to interpret the kinetics of ODN reactions. The estimated rate constants confirmed that MDC-C is the most reactive catalyst among those tested. MDC-C showed almost 2.3, 3.2, 5.1, 7.3, and 2.0 times faster kinetics in the oxidation of IND as compared to that of TiO_2-A(synth), TiO_2-A(comm.), TiO_2-R(synth.), TiO_2-R(synth.)@AC, and P-25, respectively. The turnover frequency for the oxidation of IND was estimated, which again confirmed the superiority of MDC-C in the oxidation or removal of IND. MDC-C showed higher turnover frequency than that of TiO_2-A(synth), TiO_2-A(comm.), TiO_2-R(synth.), TiO_2-R(synth.)@AC, and P-25. Moreover, the presence of additional water (5 to 10 wt% to that of acetic acid) in the solvent for the reaction slightly reduced the activity of the MDC-C for IND

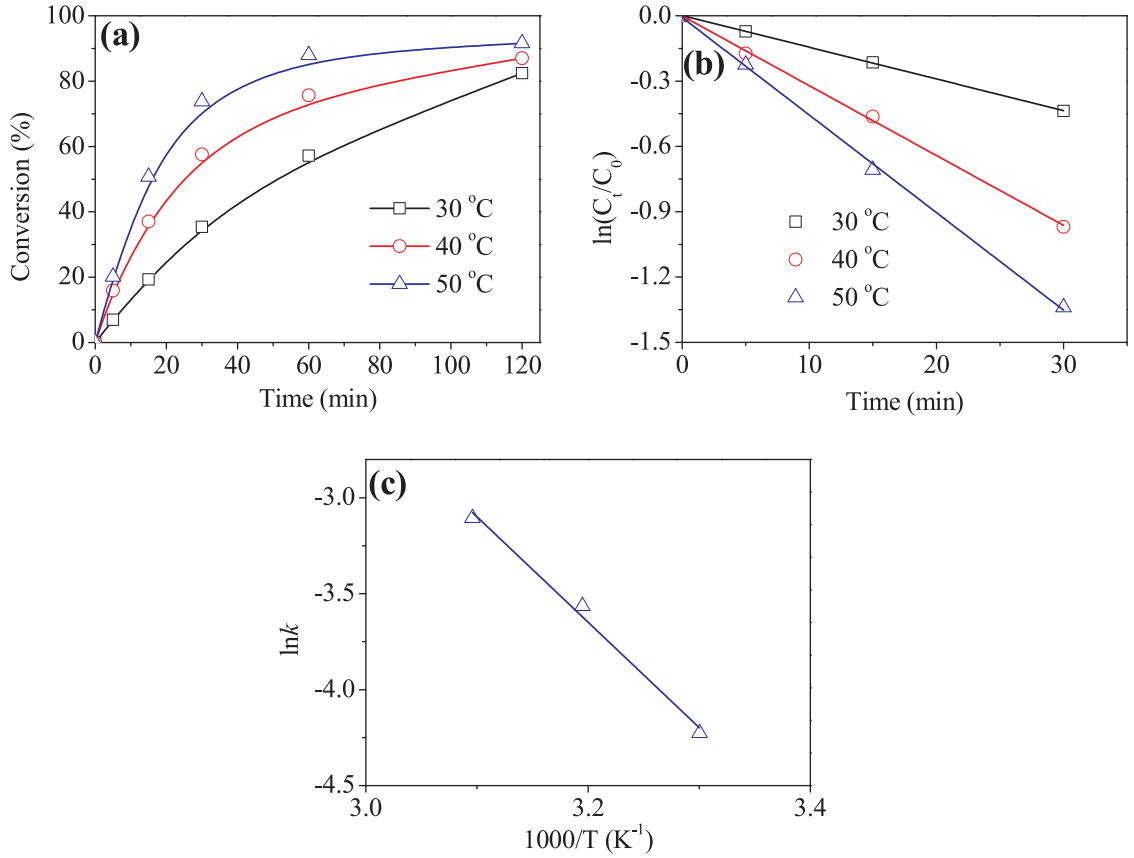

Fig. 4. Effect of reaction time on (a) IND conversion, (b) plots of the pseudo-first-order kinetics for the oxidation of IND over MDC-C at 30, 40 and 50 °C, and (c) Arrhenius plots to get the activation energies for the oxidation of IND with the MDC-C catalyst.

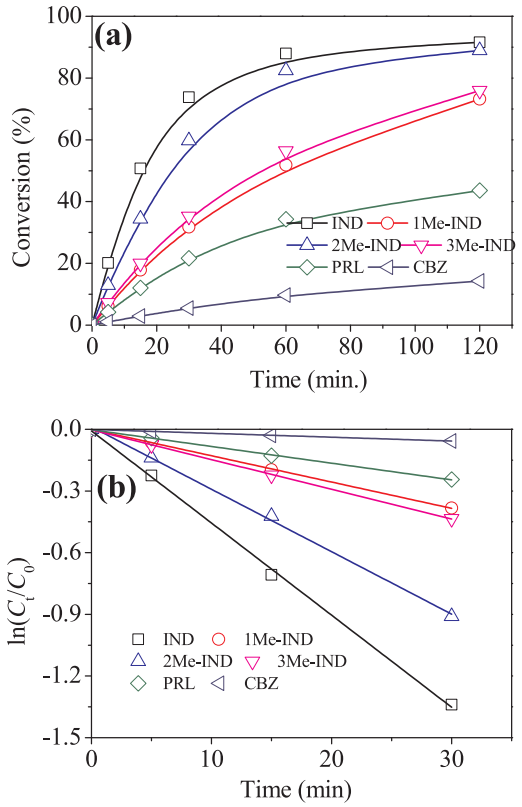

Fig. 5. Effect of reaction time on (a) conversion, (b) plots of the pseudo-first-order kinetics for the oxidation of IND, 1Me-IND, 2Me-IND, 3Me-IND, PRL and CBZ over MDC-C at 50 °C.

oxidation both in terms of conversions (Fig. S6) and reaction rates (Table 1). Therefore, it can be presumed that water has a negative effect on the oxidative removal of IND even though not very critical.

To investigate the effect of temperature as well as to estimate the activation energy for IND oxidation in the presence of MDC-C, the rate constants (k) were estimated from the reactions at three temperatures (30, 40, and 50 °C), which are compared in Fig. 4a. The results showed that the rate constants (k) summarized in Table S2, estimated from the pseudo-first-order kinetic plots (Fig. 4b), increased with increasing reaction temperature, even though the difference in the conversions was very small after the reaction for 120 min (this time is too long to compare the reactivity of the catalysts). The activation energy (E_a), estimated from the Arrhenius plot shown in Fig. 4c for the oxidation of IND, was quite low of 46 KJ·mol^{-1}. However, this value cannot be compared with others or cannot be discussed much since there was no reported value in the case of any ODN. Based on the observed results, it is suggested that IND can be removed effectively from *n*-octane by simple oxidation via H_2O_2 activation with Ti-based catalysts (especially, with MDC-C) in the presence of CH_3COOH as an extractant.

3.3. Mechanism of oxidation of ONCs

Exploration of an acceptable reaction mechanism is very important not only for the fundamental understanding of the reaction but also for possible commercialization of a developed method. For understanding the oxidation reactions of ONCs in fuels, oxidation of several IND derivatives such as 1Me-IND, 2Me-IND, and 3Me-IND, along with PRL, CBZ (other non-basic ONCs), and QUI (representative basic ONC) was conducted similarly using the MDC-C catalyst.

Fig. 5a compares the conversion of IND, 1Me-IND, 2Me-IND, 3Me-IND, PRL, and CBZ in ODN over MDC-C as a function of time. The conversion (Fig. 5a) and pseudo-first-order rate constants (Table 1), estimated from the kinetic plots shown in Fig. 5b, showed that the order of reaction in ODN was IND > 2Me-IND > 3Me-IND > 1Me-IND > PRL > CBZ. Therefore, it can be concluded that the oxidation activities of non-basic ONCs are different from one another and are dependent on the chemical structure or properties.

The GC spectra, together with the respective MS fragmentation patterns of the products, in the polar phase from the oxidation of 1Me-IND, 2Me-IND, 3Me-IND, PRL, CBZ, and QUI are shown in Figs. S7, S8, S9, S10, S11, and S12, respectively. Fig. S7a reveals the formation of three different products (named as P1, P2, and P3) by the oxidation of 1Me-IND, whereas two main products are observed from 2Me-IND (named as P1 and P2; Fig. S8a) and PRL (named as P1 and P2; Fig. S10a) oxidation. Moreover, a number of products are detected from the oxidation of 3Me-IND, whereas CBZ shows the formation of one major product (Fig. S11). On the other hand, no oxidized product is observed from QUI conversion under the studied conditions (Fig. S12). The reaction pathways can be summarized as shown in Scheme 1, based on the products. The oxidation of IND, 2Me-IND, and 3Me-IND consists of two steps; however, the oxidation of 1Me-IND proceeds in three steps. On the other hand, the oxidation of PRL occurs in a single step. However, the oxidation leads to two different products: one is the usual oxidized product (P1) (Fig. S10b) and the other is ring-opening-through-oxidation product (P2) (Fig. S10c). Moreover, all the oxidized products from Me-INDs (1Me-IND, 2Me-IND, and 3Me-IND) further undergo Baeyer-Villiger oxidation after being re-attacked by the peroxide radicals (produced from H_2O_2) [70,71]; therefore, similar products are obtained in the final stage (Scheme 1) even though 1-methylindole-2,3-dione is obtained from 1Me-IND (in the second step). In addition, CBZ is directly oxidized into 9H-carbazole-1,4-dione (Scheme 1).

For a deeper understanding of the ODN mechanism, the electron densities of the N atoms of the studied substrates are calculated by the Mulliken population analysis method, and the results are summarized in Table 2. The electron density on the N-atoms follows the order CBZ > IND > 2Me-IND > 3Me-IND > 1Me-IND > PRL > QUI. The results for the electron density on the N of INDs (IND > 2Me-IND > 3Me-IND > 1Me-IND) show that the electron density decreases (rather than the expected increase) by the introduction of the electron-donating methyl group on IND. This suggests that methyl group on IND has an electron-withdrawing character (inductive effect) rather than the expected electron-donating property, similar to a previous report [72]. More importantly, the activity of neutral ONCs (Fig. 5 and Table 1) increases with increasing electron density on the N atom of ONCs (except CBZ). Therefore, similar to the oxidation of various OSCs [32–40], ODN might also be governed by the electron density of the heteroatom (N atom) on the substrate ONCs (especially INDs). In other words, the electrophilic addition of an oxygen atom onto the substrates (via N on the ONCs) might be very important in the oxidation, similar to the ODS of OSCs [73,74]. However, it should be emphasized that the oxidizing positions (in ODN and ODS) are quite different from each other. For example, the oxidation of ODN occurs at C2 or C3 of INDs (see Scheme 1), whereas the S atom on SCCs is oxidized to sulfone (or sulfoxide) in ODS. Therefore, further work is required to understand why the electron density on N is important even though the N atom is not oxidized or attacked eventually in ODN, especially for INDs. The very low activity of CBZ (even though the electron density on the N atom is higher than that for INDs and PRL) oxidation might be explained by its chemical structure, in which oxidation, if any, can occur on the stable benzene ring [47]. The relative stability of benzene and pyrrole rings can be judged from the relative HOMO-LUMO gap, as shown in Fig. S13, in which the $\Delta E_{HOMO\ -\ LUMO}$ gaps for the pyrrole and benzene ring systems are -6.6 eV and -5.6 eV, respectively.

On the other hand, QUI was the least active or inactive (Fig. S12) in the oxidation under the studied conditions; this might be explained by the insufficient electron density on its N atom or possible poisoning of

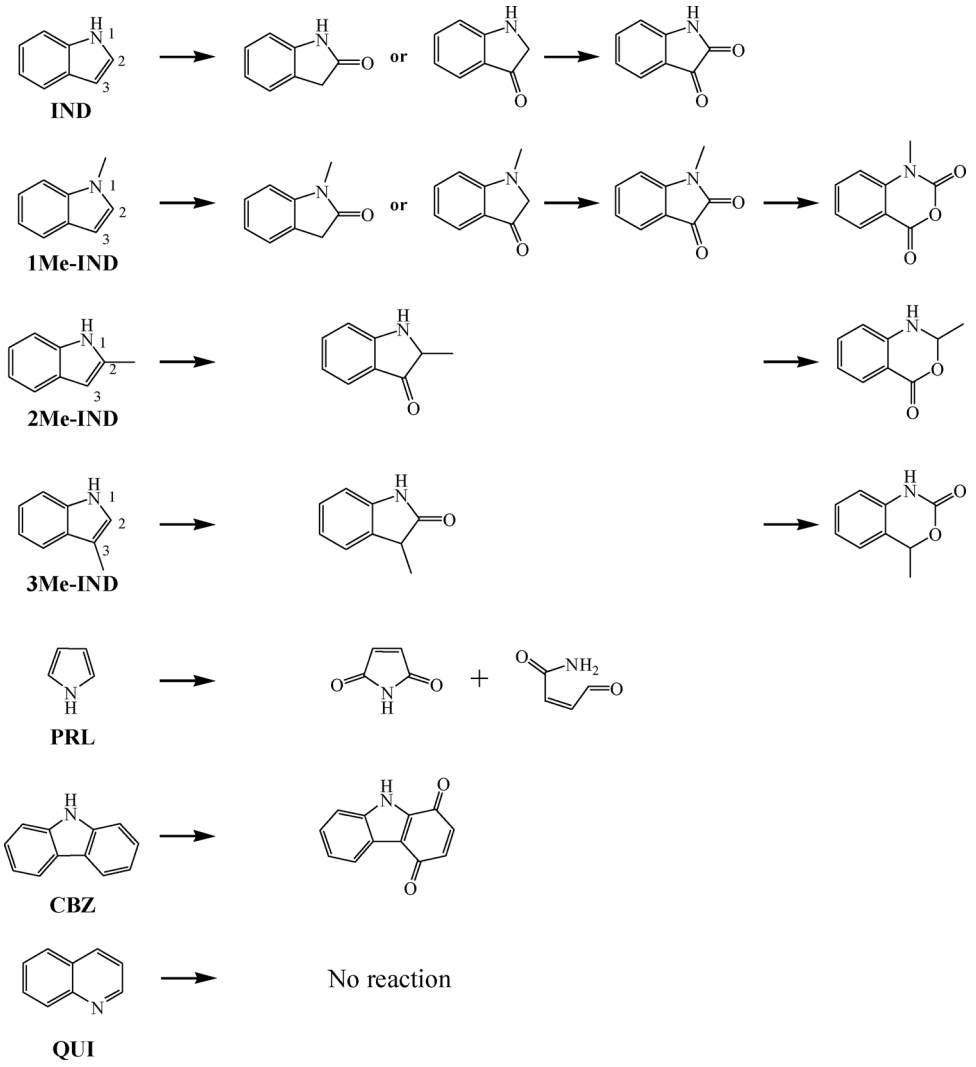

Scheme 1. Chemical structures of the studied ones and the obtained products or intermediates after oxidation reactions.

Table 2
Electron density of the N Atom in IND, 1Me-IND, 2Me-IND, 3Me-IND, PRL, CBZ and QUI calculated by mulliken method.

Substrates or ONCs	Electron density on the N atom of ONCs
IND	7.596
1Me-IND	7.471
2Me-IND	7.591
3Me-IND	7.566
CBZ	7.650
PRL	7.465
QUI	7.423

the active sites for oxidation with basic moieties such as QUI [75,76]. The low activity or high stability of QUI (which has a pyridine moiety) might also be understandable from the study [77] on the oxidation of PRL in pyridine (which was used as a solvent). However, further work is required for a clearer understanding since a recent report [54] showed the successful removal of QUI from a model fuel via ODN over a vanadium-based catalyst. In that study, quinoline-*N*-oxide was obtained from QUI and further extracted by an ionic liquid.

Therefore, it might be concluded that non-basic ONCs such as IND and Me-INDs can be effectively removed from a fuel (or *n*-octane) by oxidation with H_2O_2 over a Ti-based catalyst (MDC-C) in the presence of a suitable extractant CH_3COOH (Fig. 5). However, the conditions for ODN applied in this study were not effective for the removal of QUI from *n*-octane, partly because of the very low electron density on the N atom of QUI. Different reaction conditions were required to oxidize QUI since the ODN mechanism for basic ONCs might be quite different from that for neutral or non-basic ONCs.

3.4. Recyclability of MDC-C

The stable performance of an efficient catalyst over multiple cycles is very important and should be confirmed for commercial applications, since the operation cost can be reduced if the catalyst is reusable. The recyclability of the MDC-C catalyst in the ODN of IND was examined up to the fourth cycle (as shown in Fig. 6a) after simple solvent (acetone) washing under ultrasound sonication. The activity remained steady with only a small decrease in the subsequent cycles. Fig. 6b shows the N_2 adsorption isotherms of both the regenerated (after the second cycle) MDC-C and the fresh MDC-C; the results confirmed that the porosity remained nearly unchanged after recycling. The regenerated MDC-C had very similar crystallinity or crystal structure as that of the fresh MDC-C (Fig. 6c), also confirming the successful regeneration of the used catalyst. Therefore, the Ti-based catalyst MDC-C might be used up to several cycles in the ODN of non-basic ONCs from fuels.

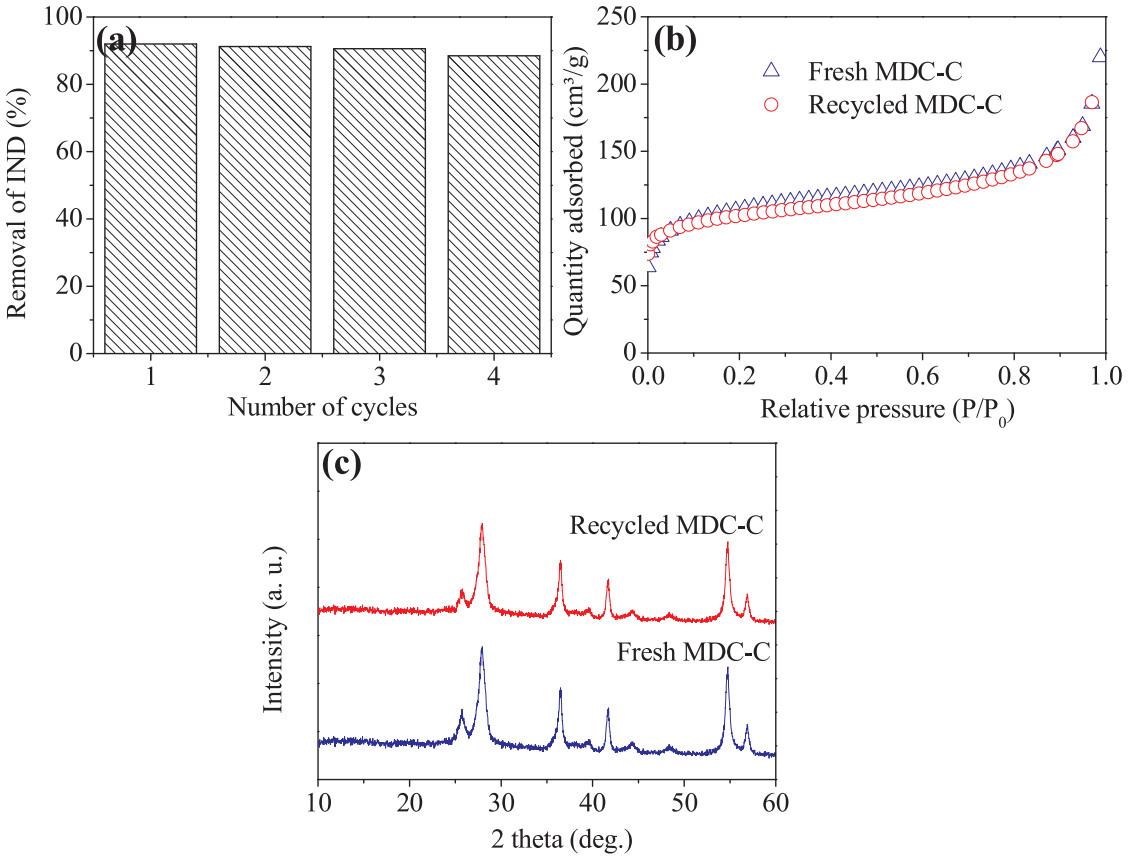

Fig. 6. (a) Recyclability of MDC-C in oxidation of IND, (b) N_2-adsorption isotherms and (c) XRD patterns of the fresh MDC-C and recycled MDC-C.

4. Conclusion

In order to understand the possible denitrogenation of fuels via a catalytic reaction, oxidation of ONCs such as IND and its derivatives in a model fuel was carried out with H_2O_2 by using uniformly dispersed TiO_2 nanoparticles in mesoporous carbon (MDC-C), obtained by the pyrolysis of an MOF composite (ZIF-8(30)@H_2N-MIL-125). The following conclusions could be drawn from this study. First, MDC-C might be a very promising catalyst in ODN based on its high porosity, large mesopore volume, high activity (or turnover frequency), and ready recyclability. Second, the oxidation rate increased with increasing electron density on the nitrogen of the INDs, suggesting the importance of the electrophilic addition of the oxygen atom onto the substrates (via N on the INDs). Third, ODN with the green oxidant H_2O_2 might be a way to remove neutral ONCs when a suitable extractant and a catalyst such as MDC-C are applied.

Notes

The authors declare no competing financial interest.

Acknowledgments

This research was supported by Basic Science Research Program through the National Research Foundation of Korea (NRF) funded by the Ministry of Science, ICT and future Planning (grant number: 2017R1A2B2008774). Authors would like to express their sincere thanks to one Reviewer who suggested oxidizing indoline.

Appendix A. Supplementary data

Supplementary material related to this article can be found, in the online version, at doi:https://doi.org/10.1016/j.apcatb.2018.09.004.

References

[1] N.L. Panwar, S.C. Kaushik, S. Kothari, Role of renewable energy sources in environmental protection: a review, Renew. Sustainable Energy Rev. 15 (2011) 1513–1524.
[2] S. Kumar, H.T. Kwon, K.H. Choi, W. Lim, J.H. Cho, K. Tak, I. Moon, LNG: an eco-friendly cryogenic fuel for sustainable development, Appl. Energy 88 (2011) 4264–4273.
[3] N. Li, X.L. Ma, Q.F. Zha, C.S. Song, Analysis and comparison of nitrogen compounds in different liquid hydrocarbon streams derived from petroleum and coal, Energy Fuels 24 (2010) 5539–5547.
[4] G.H.C. Prado, Y. Rao, A. de Klerk, Nitrogen removal from oil: a review, Energy Fuels 31 (2017) 14–36.
[5] A.M. Liaquat, M.A. Kalam, H.H. Masjuki, M.H. Jayed, Potential emissions reduction in road transport sector using biofuel in developing countries, Atmos. Environ. 44 (2010) 3869–3877.
[6] Y.Q. Jin, L. Lu, X.J. Ma, H.M. Liu, Y. Chi, K. Yoshikawa, Effects of blending hydrothermally treated municipal solid waste with coal on co-combustion characteristics in a lab-scale fluidized bed reactor, Appl. Energy 102 (2013) 563–570.
[7] G.C. Laredo, P.M. Vega-Merino, F. Trejo-Zarraga, J. Castillo, Denitrogenation of middle distillates using adsorbent materials towards ULSD production: a review, Fuel Process. Technol. 106 (2013) 21–32.
[8] H. Zhang, G. Li, Y.H. Jia, H.O. Liu, Adsorptive removal of nitrogen-containing compounds from fuel, J. Chem. Eng. Data 55 (2010) 173–177.
[9] I. Ahmed, S.H. Jhung, Adsorptive desulfurization and denitrogenation using metal-organic frameworks, J. Hazard. Mater. 301 (2016) 259–276.
[10] P. Tan, X.Y. Xie, X.Q. Liu, T. Pan, C. Gu, P.F. Chen, J.Y. Zhou, Y.C. Pan, L.B. Sun, Fabrication of magnetically responsive HKUST-1/Fe_3O_4 composites by dry gel conversion for deep desulfurization and denitrogenation, J. Hazard. Mater. 321 (2017) 344–352.
[11] N.A. Khan, S.H. Jhung, Adsorptive removal and separation of chemicals with metal-organic frameworks: contribution of π-complexation, J. Hazard. Mater. 325 (2017) 198–213.
[12] Y.X. Li, W.J. Jiang, P. Tan, X.Q. Liu, D.Y. Zhang, L.B. Sun, What matters to the adsorptive desulfurization performance of metal-organic frameworks? J. Phys. Chem. C 119 (2015) 21969–21977.
[13] Z. Hasan, S.H. Jhung, Facile method to disperse nonporous metal organic frameworks: composite formation with a porous metal organic framework and application in adsorptive desulfurization, ACS Appl. Mater. Interfaces 7 (2015)

10429–10435.
[14] I. Ahmed, N.A. Khan, J.W. Yoon, J.-S. Chang, S.H. Jhung, Protonated MIL-125-NH_2: remarkable adsorbent for the removal of quinoline and indole from liquid fuel, ACS Appl. Mater. Interfaces 9 (2017) 20938–20946.
[15] M.X. Yu, N. Zhang, L.W. Fan, C. Zhang, X.J. He, M.D. Zheng, Z. Li, Removal of organic sulfur compounds from diesel by adsorption on carbon materials, Rev. Chem. Eng. 31 (2015) 27–43.
[16] A. Rendon-Rivera, M. Cortes-Jacome, E. Lopez-Salinas, M. Mosqueira, J. Toledo-Antonio, Adsorption of nitrogen and sulphur organic-compounds on titania nanotubes, Int. J. Eng. Res. Sci. 21 (2016) 24.
[17] T. Huang, J. Xu, Y. Fan, Effects of concentration and microstructure of active phases on the selective hydrodesulfurization performance of sulfided CoMo/Al_2O_3 catalysts, Appl. Catal., B 220 (2018) 42–56.
[18] A.N. Varakin, A.V. Mozhaev, A.A. Pimerzin, P.A. Nikulshin, Comparable investigation of unsupported MoS_2 hydrodesulfurization catalysts prepared by different techniques: advantages of support leaching method, Appl. Catal., B 238 (2018) 498–508.
[19] Y. Gao, W. Han, X. Long, H. Nie, D. Li, Preparation of hydrodesulfurization catalysts using MoS_3 nanoparticles as a precursor, Appl. Catal., B 224 (2018) 330–340.
[20] P.G. Duan, P.E. Savage, Catalytic hydrothermal hydrodenitrogenation of pyridine, Appl. Catal., B 108 (2011) 54–60.
[21] C.S. Raghuveer, J.W. Thybaut, G.B. Marin, Pyridine hydrodenitrogenation kinetics over a sulphided NiMo/gamma-Al_2O_3 catalyst, Fuel 171 (2016) 253–262.
[22] H.Y. Yao, G. Wang, C.C. Zuo, C.S. Li, E.Q. Wang, S.J. Zhang, Deep hydrodenitrification of pyridine by solid catalyst coupling with ionic liquids under mild conditions, Green Chem. 19 (2017) 1692–1700.
[23] J.F. Palomeque-Santiago, R. López-Medina, R. Oviedo-Roa, J. Navarrete-Bolaños, R. Mora-Vallejo, J.A. Montoya-de la Fuente, J.M. Martínez-Magadán, Deep oxidative desulfurization with simultaneous oxidative denitrogenation of diesel fuel and straight run gas oil, Appl. Catal., B 236 (2018) 326–337.
[24] X.C. Chen, S. Yuan, A.A. Abdeltawab, S.S. Al-Deyab, J.W. Zhang, L. Yu, G.R. Yu, Extractive desulfurization and denitrogenation of fuels using functional acidic ionic liquids, Sep. Purif. Technol. 133 (2014) 187–193.
[25] R. Abro, M. Abro, S.R. Gao, A.W. Bhutto, Z.M. Ali, A. Shah, X.C. Chen, G.R. Yu, Extractive denitrogenation of fuel oils using ionic liquids: a review, RSC Adv. 6 (2016) 93932–93946.
[26] X. Feng, X.L. Ma, N. Li, C. Shang, X.M. Yang, X.D. Chen, Adsorption of quinoline from liquid hydrocarbons on graphite oxide and activated carbons, RSC Adv. 5 (2015) 74684–74691.
[27] X. Han, H.F. Lin, Y. Zheng, The role of oxygen functional groups in the adsorption of heteroaromatic nitrogen compounds, J. Hazard. Mater. 297 (2015) 217–223.
[28] D. Liu, J.Z. Gui, Z.L. Sun, Adsorption structures of heterocyclic nitrogen compounds over Cu(I)Y zeolite: a first principle study on mechanism of the denitrogenation and the effect of nitrogen compounds on adsorptive desulfurization, J. Mol. Catal. A Chem. 291 (2008) 17–21.
[29] A. Koriakin, K.M. Ponvel, C.H. Lee, Denitrogenation of raw diesel fuel by lithium-modified mesoporous silica, Chem. Eng. J. 162 (2010) 649–655.
[30] L.L. Xie, A. Favre-Reguillon, X.X. Wang, X.Z. Fu, M. Lemaire, Selective adsorption of neutral nitrogen compounds from fuel using ion-exchange resins, J. Chem. Eng. Data 55 (2010) 4849–4853.
[31] W. Chaikittisilp, K. Ariga, Y. Yamauchi, A new family of carbon materials: synthesis of MOF-derived nanoporous carbons and their promising applications, J. Mater. Chem. A 1 (2013) 14–19.
[32] S.N. Wei, H.J. He, Y. Cheng, C.P. Yang, G.M. Zeng, L. Qiu, Performances, kinetics and mechanisms of catalytic oxidative desulfurization from oils, RSC Adv. 6 (2016) 103253–103269.
[33] C.N. Dai, J. Zhang, C.P. Huang, Z.G. Lei, Ionic liquids in selective oxidation: catalysts and solvents, Chem. Rev. 117 (2017) 6929–6983.
[34] M.H. Ibrahim, M. Hayyan, M.A. Hashim, A. Hayyan, The role of ionic liquids in desulfurization of fuels: a review, Renew. Sustainable Energy Rev. 76 (2017) 1534–1549.
[35] P.S. Kulkarni, C.A.M. Afonso, Deep desulfurization of diesel fuel using ionic liquids: current status and future challenges, Green Chem. 12 (2010) 1139–1149.
[36] C. Shen, Y.J. Wang, J.H. Xu, G.S. Luo, Oxidative desulfurization of DBT with H_2O_2 catalysed by TiO_2/porous glass, Green Chem. 18 (2016) 771–781.
[37] Z. Ismagilov, S. Yashnik, M. Kerzhentsev, V. Parmon, A. Bourane, F. Al-Shahrani, A. Hajji, O. Koseoglu, Oxidative desulfurization of hydrocarbon fuels, Catal. Rev. Sci. Eng. 53 (2011) 199–255.
[38] J. Kim, N.D. McNamara, T.H. Her, J.C. Hicks, Carbothermal reduction of Ti-modified IRMOF-3: an adaptable synthetic method to support catalytic nanoparticles on carbon, ACS Appl. Mater. Interfaces 5 (2013) 11479–11487.
[39] J.M. Fraile, C. Gil, J.A. Mayoral, B. Muel, L. Roldán, E. Vispe, S. Calderón, F. Puente, Heterogeneous titanium catalysts for oxidation of dibenzothiophene in hydrocarbon solutions with hydrogen peroxide: on the road to oxidative desulfurization, Appl. Catal., B 180 (2016) 680–686.
[40] A. Bazyari, A.A. Khodadadi, A.H. Mamaghani, J. Beheshtian, L.T. Thompson, Y. Mortazavi, Microporous titania–silica nanocomposite catalyst-adsorbent for ultra-deep oxidative desulfurization, Appl. Catal., B 180 (2016) 65–77.
[41] K. Chen, N. Liu, M. Zhang, D. Wang, Oxidative desulfurization of dibenzothiophene over monoclinic VO_2 phase-transition catalysts, Appl. Catal., B 212 (2017) 32–40.
[42] M. Craven, D. Xiao, C. Kunstmann-Olsen, E.F. Kozhevnikova, F. Blanc, A. Steiner, I.V. Kozhevnikov, Oxidative desulfurization of diesel fuel catalyzed by polyoxometalate immobilized on phosphazene-functionalized silica, Appl. Catal., B 231 (2018) 82–91.
[43] K.H. Chu, Y.A. Al-Hamadani, C.M. Park, G. Lee, M. Jang, A. Jang, N. Her, A. Son, Y. Yoon, Ultrasonic treatment of endocrine disrupting compounds, pharmaceuticals, and personal care products in water: a review, Chem. Eng. J. 327 (2017) 629–647.
[44] K.Y.A. Lin, J.T. Lin, H.T. Yang, Ferrocene-modified chitosan as an efficient and green heterogeneous catalyst for sulfate-radical-based advanced oxidation process, Carbohydr. Polym. 173 (2017) 412–421.
[45] S.B. Hammouda, N. Adhoum, L. Monser, Chemical oxidation of a malodorous compound, indole, using iron entrapped in calcium alginate beads, J. Hazard. Mater. 301 (2016) 350–361.
[46] Y. Shiraishi, K. Tachibana, T. Hirai, I. Komasawa, A novel desulfurization process for fuel oils based on the formation and subsequent precipitation of S-alkylsulfonium salts. 3. Denitrogenation behavior of light oil feedstocks, Ind. Eng. Chem. Res. 40 (2001) 3390–3397.
[47] Y. Shiraishi, K. Tachibana, T. Hirai, I. Komasawa, Desulfurization and denitrogenation process for light oils based on chemical oxidation followed by liquid-liquid extraction, Ind. Eng. Chem. Res. 41 (2002) 4362–4375.
[48] A. Ishihara, D.H. Wang, F. Dumeignil, H. Amano, E.W.H. Qian, T. Kabe, Oxidative desulfurization and denitrogenation of a light gas oil using an oxidation/adsorption continuous flow process, Appl. Catal., A 279 (2005) 279–287.
[49] X. Zhou, H. Ma, X. Fu, C. Yao, J. Xiao, Catalytic oxidation of carbazole using t-butyl hydroperoxide over molybdenum catalysts, J. Fuel Chem. Technol. 38 (2010) 75–79.
[50] L. da Conceicao, C.L. de Almeida, S. Egues, R.M. Dallago, N. Paroul, I. do Nascimento, W.F. de Souza, S.B.C. Pergher, Preliminary study of the oxidation of nitrogen compounds of gas oil from Brazilian petroleum, Energy Fuels 19 (2005) 960–963.
[51] D. Carnaroglio, E.C. Gaudino, S. Mantegna, E.M. Moreira, A.V. de Castro, E.M.M. Flores, G. Cravotto, Ultrasound-assisted oxidative desulfurization/denitrification of liquid fuels with solid oxidants, Energy Fuels 28 (2014) 1854–1859.
[52] Z. Hu, H. Yu, Oxidative denitrification of diesel by phosphomolybdic acid/hydrogen peroxide, Pet. Sci. Technol. 33 (2015) 968–974.
[53] Z. Hu, H.L. Yu, Ultrasound assisted oxidative denitrification of diesel by formic acid/hydrogen peroxide, Pet. Sci. Technol. 34 (2016) 268–273.
[54] A.S. Ogunlaja, O.S. Alade, Catalysed oxidation of quinoline in model fuel and the selective extraction of quinoline-N-oxide with imidazoline-based ionic liquids, Egypt. J. Pet. 27 (2018) 159–168.
[55] A.S. Ogunlaja, M.S. Abdul-quadir, P.E. Kleyi, E.E. Ferg, P. Watts, Z.R. Tshentu, Towards oxidative denitrogenation of fuel oils: vanadium oxide-catalysed oxidation of quinoline and adsorptive removal of quinoline-N-oxide using 2,6-pyridine-polybenzimidazole nanofibers, Arabian J. Chem. (2017), https://doi.org/10.1016/j.arabjc.2017.05.010.
[56] B.N. Bhadra, J.Y. Song, N.A. Khan, S.H. Jhung, TiO_2-containing carbon derived from a metal-organic framework composite: a highly active catalyst for oxidative desulfurization, ACS Appl. Mater. Interfaces 9 (2017) 31192–31202.
[57] S.D. Bishopp, J.L. Scott, L. Torrente-Murciano, Insights into biphasic oxidations with hydrogen peroxide; towards scaling up, Green Chem. 16 (2014) 3281–3285.
[58] Y.Y. Liang, H.L. Wang, H.S. Casalongue, Z. Chen, H.J. Dai, TiO_2 nanocrystals grown on graphene as advanced photocatalytic hybrid materials, Nano Res. 3 (2010) 701–705.
[59] M. Anwar, S. Kumar, F. Ahmed, N. Arshi, C.G. Lee, B.H. Koo, One step synthesis of rutile TiO2 nanoparticles at low temperature, J. Nanosci. Nanotechnol. 12 (2012) 1555–1558.
[60] R. Mulliken, Criteria for the construction of good self-consistent-field molecular orbital wave functions, and the significance of lCAO-MO population analysis, J. Chem. Phys. 36 (1962) 3428–3439.
[61] N. Uddin, C.H. Choi, Comparative atomic charges on Na^+-(H_2O) n (n= 1–6) clusters, Bull. Korean Chem. Soc. 36 (2015) 827–831.
[62] M.W. Schmidt, K.K. Baldridge, J.A. Boatz, S.T. Elbert, M.S. Gordon, J.H. Jensen, S. Koseki, N. Matsunaga, K.A. Nguyen, S. Su, General atomic and molecular electronic structure system, J. Comput. Chem. 14 (1993) 1347–1363.
[63] X. Li, H. Lin, X. Chen, H. Niu, T. Zhang, J. Liu, F. Qu, Fabrication of TiO_2/porous carbon nanofibers with superior visible photocatalytic activity, New J. Chem. 39 (2015) 7863–7872.
[64] A. Corma, M. Diaz-Cabanas, J. Martinez-Triguero, F. Rey, J. Rius, A large-cavity zeolite with wide pore windows and potential as an oil refining catalyst, Nature 418 (2002) 514–517.
[65] D. Sawant-Dhuri, V.V. Balasubramanian, K. Ariga, D.H. Park, J.H. Choy, W.S. Cha, S.S. Al-deyab, S.B. Halligudi, A. Vinu, Titania nanoparticles stabilized HPA in SBA-15 for the intermolecular hydroamination of activated olefins, ChemCatChem 6 (2014) 3347–3354.
[66] V. Malgras, Q. Ji, Y. Kamachi, T. Mori, F.-K. Shieh, K.C.-W. Wu, K. Ariga, Y. Yamauchi, Templated synthesis for nanoarchitectured porous materials, Bull. Chem. Soc. Jpn. 88 (2015) 1171–1200.
[67] Q.-L. Zhu, Q. Xu, Immobilization of ultrafine metal nanoparticles to high-surface-area materials and their catalytic applications, Chem 1 (2016) 220–245.
[68] S.B. Khomane, D.S. Doke, M.K. Dongare, S.B. Halligudi, S.B. Umbarkar, Efficient oxidation of ethyl benzene using in situ generated molybdenum acetylide oxo-peroxo complex as recyclable catalyst, Appl. Catal. A Gen. 531 (2017) 45–51.
[69] Y. Zi, Z.J. Cai, S.Y. Wang, S.J. Ji, Synthesis of isatins by I_2/TBHP mediated oxidation of indoles, Org. Lett. 16 (2014) 3094–3097.
[70] K. Neimann, R. Neumann, Electrophilic activation of hydrogen peroxide: selective oxidation reactions in perfluorinated alcohol solvents, Org. Lett. 2 (2000) 2861–2863.
[71] M. Uyanik, K. Ishihara, Baeyer-villiger oxidation using hydrogen peroxide, ACS Catal. 3 (2013) 513–520.
[72] N. Otero, M. Mandado, R.A. Mosquera, Nucleophilicity of indole derivatives: activating and deactivating effects based on proton affinities and electron density

properties, J. Phys. Chem. A 111 (2007) 5557–5562.
[73] S. Otsuki, T. Nonaka, N. Takashima, W.H. Qian, A. Ishihara, T. Imai, T. Kabe, Oxidative desulfurization of light gas oil and vacuum gas oil by oxidation and solvent extraction, Energy Fuels 14 (2000) 1232–1239.
[74] Z. Hasan, J. Jeon, S.H. Jhung, Oxidative desulfurization of benzothiophene and thiophene with WO_x/ZrO_2 catalysts: effect of calcination temperature of catalysts, J. Hazard. Mater. 205 (2012) 216–221.
[75] C. Kwak, J.J. Lee, J.S. Bae, S.H. Moon, Poisoning effect of nitrogen compounds on the performance of $CoMoS/Al_2O_3$ catalyst in the hydrodesulfurization of dibenzothiophene, 4-methyldibenzothiophene, and 4,6-dimethyldibenzothiophene, Appl. Catal. B (35) (2001) 59–68.
[76] L. Cedeño Caero, F. Jorge, A. Navarro, A. Gutiérrez-Alejandre, Oxidative desulfurization of synthetic diesel using supported catalysts: part II. Effect of oxidant and nitrogen-compounds on extraction–oxidation process, Catal. Today 116 (2006) 562–568.
[77] J.K. Howard, K.J. Rihak, A.C. Bissember, J.A. Smith, The oxidation of pyrrole, Chem. Asian J. 11 (2016) 155–167.